Research in Molecular Medicine

The Possibility of Destruction of Cellular NADPH in the Presence of Free Fe(II) Ion, Arsine, and Other Hazardous Species

Seyyed Amir Siadati[1*], **Mohammad Ali Ebrahimzadeh**[2*], **Esmaeil Babanezhad**[3]

1. Pharmaceutical Sciences Research Center, Hemoglobinopathy Institute, Mazandaran University of Medical Sciences, Sari, Iran.
2. Department of Medicinal Chemistry, Pharmaceutical Sciences Research Center, School of Pharmacy, Mazandaran University of Medical Sciences, Sari, Iran.
3. Department of Environmental Health, Faculty of Health, Mazandaran University of Medical Sciences, Sari, Iran.

Use your device to scan and read the article online

Citation Siadati SS, Ebrahimzadeh MA, Ebrahimzadeh E. The Possibility of Destruction of Cellular NADPH in the Presence of Free Fe(II) Ion, Arsine, and Other Hazardous Species. Research in Molecular Medicine. 2022; 10(4):215-224. https://doi.org/10.32598/rmm.10.4.11.24

https://doi.org/10.32598/rmm.10.4.11.24

Article Type:
Research Paper

Article info:
Received: 14 Sep 2022
Revised: 30 Sep 2022
Accepted: 17 Oct 2022

Keywords:
NADPH, Iron overload, Arsine, Free Fe(II), Decomposition, Density functional theory

ABSTRACT

Background: As the nicotinamide adenine dinucleotide phosphate (NADPH) is the key natural electron generator of the alive cells, investigation of the possibility of inactivation or even destruction of it by hazardous chemical molecules or ions seems to be very important.

Methods: Due to this, in this project, the behavior of NADPH in the presence of some chemical species containing Fe(II) ion, arsine, phosphoric acid, and some low weight alcohols have been investigated by using the density functional theory (DFT) method.

Results: Comparison of the results of the potential energy surface (PES) study showed that adsorption of methanol, ethanol, normal propanol, H3PO4, arsine and Fe(II) ion by NADPH release -23.19 kcal mol-1, -23.03 kcal mol-1, -23.30 kcal mol-1, -35.04 kcal mol-1, -53.03 kcal mol-1, and -161.59 kcal mol-1 energy, respectively.

Conclusion: It indicates that absorption, and even destruction of NADPH by a free Fe(II) ion is very favorable in view of thermodynamics. Somehow, such energy release could make this process irreversible. Also, the geometrical results show that during the adsorption of iron ion by the NADPH, the phosphate bridge breaks and the molecule decompose in two different parts.

*** Corresponding Authors:**
Seyyed Amir Siadati
Address: *Pharmaceutical Sciences Research Center, Hemoglobinopathy Institute, Mazandaran University of Medical Sciences, Sari, Iran.*
Phone: *+98 (938) 1098730*
E-mail: *Chemistry_@021@yahoo.com*

Mohammad Ali Ebrahimzadeh*, Professor.*
Address: *Department of Medicinal Chemistry, Pharmaceutical Sciences Research Center, School of Pharmacy, Mazandaran University of Medical Sciences, Sari, Iran.*
Phone: *+98 (911) 1541214*
E-mail: *MA.Ebrahimzadeh@mazums.ac.ir*

Introduction

Diseases related to iron overload, such as early-onset Alzheimer [1], heart failure [2], and Parkinson [3], have recently been topics for hot debates among researchers [4-6]. Recent reports emphasize that although cells need a certain amount of iron, the excess concentration of this element could result in severe diseases and organ failure. Moreover, the role of excess iron ions in generating free radical species (which could decompose many important biological molecules and destroy tissues) has been investigated [7, 8]. Accordingly, many scientists worldwide have performed valuable research to find ways to eliminate excess iron from the body [9-12].

The nicotinamide adenine dinucleotide phosphate (NADPH) is a key electron generator in living organisms on our planet. It provides the required electrons for biological reducing processes that drive numerous anabolic reactions, especially those responsible for the biosynthesis of all significant cell molecules [13, 14]. Thus, NADPH and its functions are essential for the survival of the complex life of earth, our beautiful, fragile home.

It is evident that, on the one hand, iron is essential for the survival of the cells, while, on the other hand, it is highly oxidative and could produce dangerous reactive oxygen species (in its overload states). In other words, the range of iron concentration in the cells and biological systems is narrow for its optimized beneficial effects (and minimized toxic behavior). Thus, understanding the mechanism of controlling iron in the tissues is very important. In this regard, some previous studies reveal that the level of ferritin (an iron-storage protein of cells) between the cell walls rises under conditions of excess iron [15]. Thus, when the concentration of iron ions rises in an iron overload system, it is stored in an inert form. It should be noted that Fe(II) is active while Fe(III) is inert. When an electron is released from the system, Fe(II) turns into Fe(III), and when an electron is gained, Fe (III) becomes Fe(II). Also, the ferritin collects iron ions only in the form of Fe (III). Thus, the ferritin level rises to absorb iron in Fe(III) form in an iron-overloaded system. Therefore, the excess iron does not usually intervene in generating reactive oxygen [16, 17]. However, some key molecules will be targeted if free Fe(II) ions exist in the system in high iron overload conditions. The results of our work indicate that free Fe(II) could decompose the NADPH agent by breaking its phosphate bridge. Some reports which could support this result are as follows.

For example, in an in vitro experiment, Petrat et al. stated that nicotinamide adenine dinucleotide (NADH) could be oxidized by Iron ions (probably via its phosphate part) [18]. The related studies also emphasize that phosphate could compete with iron ion chelators in making metal complexes [18-20]. More interestingly, precipitation occurs during the mixing of the phosphate buffer with ferric phenanthroline [21], which affects the Fe assay (II).

In another work, Minotti and Ikeda-Saito found a microsomal iron protein that provokes NADPH oxidation by transferring the electron density from NADPH-cytochrome P450 reductase to the Fe(III) bond [22]. They also revealed that detergents perform the related experiment for Fe(II) to cease the oxidative incorporation of iron that did not react with NADPH-cytochrome P450 reductase [23]. Also, Sijmons et al. revealed that the NADPH species is an electron donor agent for the high Fe(III) ion reduction found in iron-deficient roots [24].

It is worth saying that the density functional theory (DFT) method (especially at the B3LYP level of theory) has widely been used for potential energy surface (PES) calculation [25-29] and adsorption process estimations [30-32]. As a closed example, researchers have studied the structures, UV–visible spectra, and also the oxidation mechanism of NADPH and NADP+ species by using the DFT method [33]. Also, a group of scientists have studied on the polystyrene-based eosin-Y as the photocatalyst agent for light-mediated NADH/NADPH system by DFT method [34]. Moreover, another group of scientists studied the hydride transfer of NADPH by applying this valuable theoretical approach [35].

Thus, due to the key role of NADPH natural electron generator in the energy cycle of the alive cells on the one hand and the importance of iron overload diseases on the other hand, in this work, the behavior of NADPH in the presence of Fe(II) ion, as well as some other chemical species containing arsine, phosphoric acid, and some of the low-weight alcohols have been investigated by the DFT approach. This study showed that the adsorption energy difference of Fe(II) ion is significantly higher than all other species (especially those of alcohol). It confirms that NADPH's absorption (and even destruction) by a free Fe(II) ion is very favorable in view of thermodynamics. Somehow, such energy release could make this process irreversible. In addition, the geometrical results show that during the adsorption of iron ions by the NADPH, the phosphate bridge breaks, and the molecule decomposes into two parts. It would be another proof of the toxicity of free iron ions and, perhaps, iron overload.

Computational details

All calculations were done using the Gaussian 03 chemical quantum package [36]. The structural geometries for each critical structure were optimized by applying the DFT approach at the B3LYP/6-311G(d, p) level of theory [37-39]. The same techniques were recently used to study the mechanical aspects of several adsorption processes [40-42]. In addition, the global electron density transfer (GEDT) [43] has been extracted by the Equation 1:

1. $GEDT=|\Sigma q_A|$,

where q_A is the net Mulliken charge and the sum of all the atoms of the adsorbed species before the adsorption process. Also, Δ (e) is the total charge transfer of the small chemical agent, calculated by the Equation 2:

2. $\Delta(e)=GEDT_{Ads}-GEDT_{Iso}$,

where $GEDT_{Ads}$ is the GEDT of adsorbed species, and $GEDT_{Iso}$ is the GEDT of adsorbed species in its isolated form (before adsorption).

The chemical potential of each system, or the Fermi level (E_F), has been calculated by the Equation 3 [44]:

3. $E_F=-(E_{HOMO}+E_{LUMO})/2$,

where E_{HOMO} and E_{LUMO} are the energy content of HOMO and LUMO, respectively. Moreover, the energy gaps E_gs were calculated by applying the Equation 4 [45]:

4. $E_g=(E_{LUMO}-E_{HOMO})$.

In addition, the energy of adsorption (E_{ads}) has been calculated by the Equation 5:

5. $E_{ads}=E_{sys}-(E_{sorbent}+E_{IAS})$,

where E_{sys} is the potential energy of the system, Es_{orbent} is the potential energy of the isolated sorbent, and E_{IAS} is the potential energy of the isolated adsorbed species before the adsorption process. Also, the natural bond orbital [46] was used to support the results of the GEDT data. Moreover, the key reactivity descriptors for NADPH molecule were calculated by the Equations 6, 7, 8 and 9 [47-50]:

6. Global hardness (η)=(I-A)/2;

7. Softness (S)=1/2η (7);

8. Electronegativity (χ)=(I+A)/2;

9. Electrophilicity index ($\omega=\mu^2/2\eta$),

where I refers to the negative of the HOMO energy level ($-E_{HOMO}$), A denotes the negative of the LUMO energy level ($-E_{LUMO}$), and also μ is the chemical potential which is defined as (Equation 10):

10. $\mu=(I+A)/2$.

Results

Each of the considered species containing NADPH, Fe(II), arsine, H_3PO_4, methanol, ethanol, and normal propanol were prepared as input files and then placed under the optimization step to the B3LYP/6-311G(d, p) level of theory to give the relatively more stable geometries. Next, each considered species containing Fe(II), arsine, H_3PO_4, methanol, ethanol, and normal propanol were put in different positions near the NADPH to give the most reliable local energy minima. The results of the calculation process showed that in the case of alcohols, the difference in the energy of adsorption E_{ads} is much lower than those of other considered cases (especially lower than the Fe(II) case). Considering thermodynamics, it shows that the adsorption (and destruction) of Fe(II) with NADPH is more favorable than those of alcohols.

Figure 1 shows the optimized structures of the isolated NADPH and its complex, with each mentioned species containing alcohols, phosphoric acid, arsine, and Fe(II) ions. This figure shows that the isolated NADPH contains a nicotinamide part linked to an adenosine-like segment via the phosphate bridge. The local energy minima for the isolated NADPH reached from the optimization processes show that this molecule has a stable twisted structure due to its polar atomic interactions and hydrogen bonding between the two heads of the molecule. For example, the distances of the hydrogen bonding between O(57)···H(28) and O(58) ···H(26), which link the two heads of the NAPDH, are 1.64 and 1.77 Å, respectively. On the other hand, the distances between the Na(77) atom of the phosphate and the O(25) and O(27) atoms of the nicotinamide part are 2.42 and 2.44 Å, respectively, indicating the strong interactions between the two heads of NADPH, leading to its twisted structure. Also, the degree of the dihedral angle of the two arms of the phosphate bridge is about 21.9° for O(32)-P(33)-P(37)-O(40), which indicates its closed angle. Perhaps these atomic links have stabilized such a wrapped molecular system. In the case of the methanol-NADPH system, it

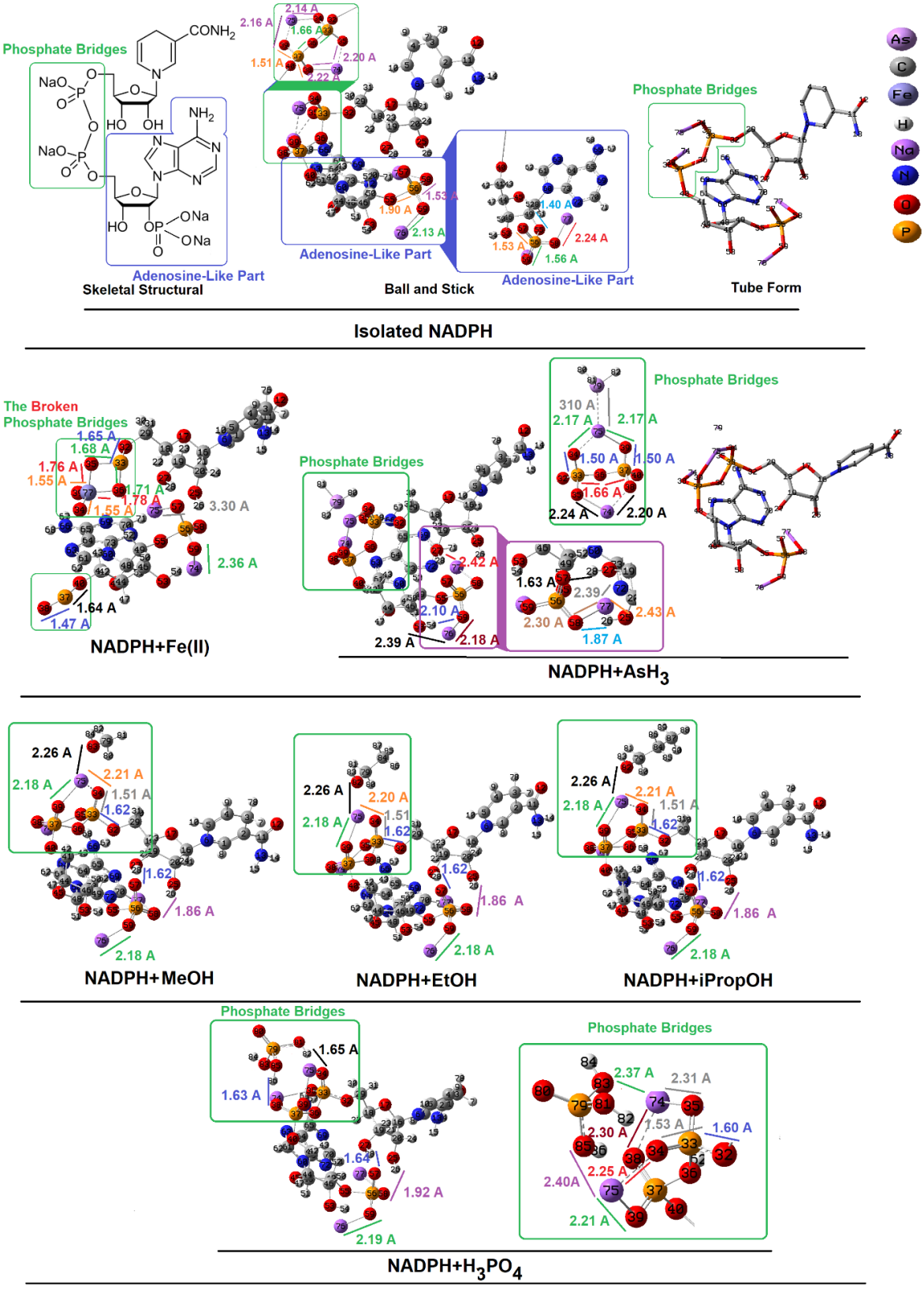

Figure 1. The geometrical structures of the isolated NADPH and its complexes with the considered species, optimized at B3LYP/6-311G(d, p) level of theory

Table 1. The key thermodynamic and structural parameters of each isolated or complex system

Species	NADPH	NADPH-Fe(II)	NADPH-AsH_3	NADPH-MeOH	NADPH-EtOH	NADPH-ProOH	NADPH+H_3PO_4
ΔE	-	-161.59	-53.03	-23.19	-23.02	-23.30	-35.04
Δ (e)	-	-0.56	0.18	-0.22	0.07	0.07	0.00
DM (D)	13.28	6.22	8.34	7.93	7.71	7.56	10.8
Q_m	-	1.44	-0.06	-	-	-	1.26
X-NADPH	-	1.56	3.11	2.26	2.26	2.26	1.62

Note: ΔE (kcal/mol): Energy difference; Δ (e): Total charge transfer of the small chemical agent, DM (D): Dipole moment; Q_m (e): Atomic charge of the metal; X-NADPH (Å): Distance between the small chemical species and the NADPH.

could be observed that the interaction between the oxygen atom of methanol (O 83) and the sodium atom of NADPH (Na 75) (with a distance of 2.26 Å) has made a stable local energy minimum. The dihedral angle of the two arms of the phosphate bridge in this system is about 13.5° for O(32)-P(33)-P(37)-O(40), which shows a slight deviation from the dihedral angle of the isolated system. Moreover, the lengths of the hydrogen bonds for O(57)···H(28), and O(58) ···H(26), which link the two heads of the NAPDH, are 1.62 and 1.86 Å, respectively. Thus, the distance between the two heads of the molecule has not deviated from the isolated structure.

In the cases of the two remaining alcohols containing ethanol and normal propanol, their distances with NADPH equal 2.26 Å. Also, as shown in Figure 1, most of the atomic distances, especially the O(57)···H(28), and O(58) ···H(26) (which are related to the distances between the two heads of the NADPH molecules) are very closed to the methanol-NADPH system. These observations agree with the outcome of the PES calculations, which reveal the very closed energy release values during the adsorption processes of each of the three alcohols by NADPH.

However, in the case of H_3PO_4, the interactions are more complicated than the alcohols. Somehow, there are two intermolecular hydrogen bonds and two Na···O gravitations. More precisely, after adsorption of H_3PO_4 by NADPH, two H bonds containing O(34)···H(82) (1.65 Å), and O(38)···H(36) (1.63 Å), and two polar atomic interactions containing Na(74)···O(83) (2.37 Å), and Na(75)···O(85) (2.40 Å) are formed. Moreover, the value of the dihedral angle of O(32)- P(33)-P(37)-O(40) reaches 47.9° which is higher than that of alcohols. However, the lengths of O(57)···H(28) and O(58)···H(26) hydrogen bonds reach 1.64 and 1.92 Å, which have no significant differences with the alcohol cases. The formation of four strong interactions in the H_3PO_4-NADPH system, compared to only one intermolecular interaction in each of the alcohols, is the reason for a higher amount of its energy release during the adsorption.

The process of adsorption of arsine chemical species (AsH_3) by NADPH is somewhat different from the processes mentioned above (containing the alcohols and H_3PO_4). To be more precise, the distance between As(79) and Na(75), which represents the intermolecular space between arsine and NADPH, is about 3.11 Å (Table 1). Moreover, like the previously mentioned systems, in the geometrical structure of the local energy minimum of this case, the pathogen species is near the phosphate bridge. Also, replacing arsine with the other mentioned species has not affected the distances of two heads of NADPH. In this system, the hydrogen bond lengths of O(57)···H(28), and O(58) ···H(26) are 1.63 and 1.87 Å, respectively, which are very close to the other mentioned systems. Interestingly, the dihedral angle of O(32)-P(33)-P(37)-O(40) is about 12.6°, which shows a slight deviation from the isolated system.

This study might be more interesting when investigating the Fe(II)-NADPH complex. Because, in this case, most of the focused parameters change. The most important change that occurs during the adsorption of Fe(II) is the breaking of the phosphate bridge of NADPH. Somehow, Fe(II) ion breaks the O(36)-P(37), O(34)-P(33), and O(39)-P(37) bonds on the one hand and forms the O(34)-Fe(77) (1.55 Å), O(35)-Fe(77) (1.76 Å), O(36)-Fe(77) (1.78 Å), and O(39)-Fe(77) (1.55 Å) bonds, on the other hand. By these changes, the dihedral angle of O(32)-P(33)-P(37)-O(40) does not exist anymore. Moreover, the system's dipole moment (DM) changes from 13.28 in the isolated NADPH to 6.22 in the Fe(II) contaminated system. Also, the amount of DM in Fe(II)-NADPH complex is less than all of the other systems

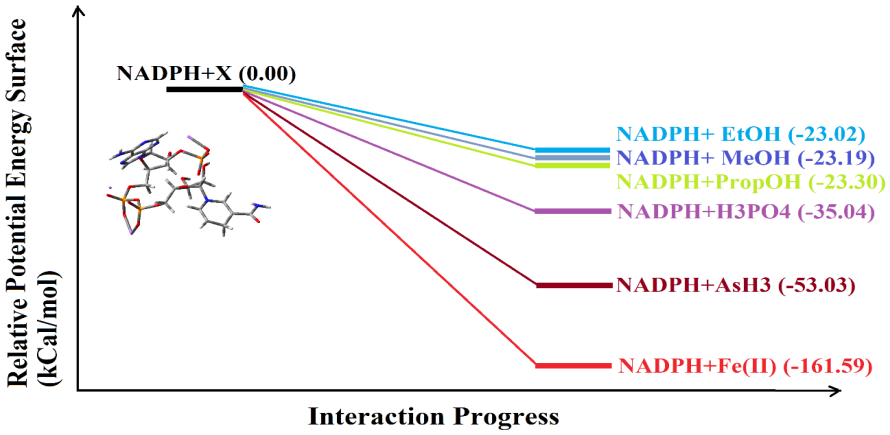

Figure 2. The related PES of the interaction between NADPH with the considered species at B3LYP/6-311G(d, p) level

containing AH_3 (DM=8.34), H_3PO_4 (DM=10.8), MeOH (DM=7.93), EtOH (7.71), and ProOH (7.56), which show considerable changes on the NADPH system after absorption of free Fe(II) ion. In addition, the Q_m (total charge of the metal) in the Fe(II)-NADPH is about 1.44, which indicates this atom has received a -0.56 electron charge from NADPH, and thus, this ion has oxidized that molecule.

Figure 2 and Table 1 show that during the adsorption interaction of methanol, ethanol, and normal propanol by NADPH, -23.02, -23.19, and -23.30 kcal/mol energies are released from the system, respectively. It shows that changes in the alkyl chain of those alcohols do not alter the adsorption energy compared to the other cases. Also, the same distances between the O atoms of the considered alcohols and the sodium atoms of the NADPH (about 2.26 Å in Figure 1) would confirm such closed E_{adss}. In the case of adsorption of H_3PO_4, a -35.04 kcal/mol energy is released, and its energy difference is about -12 kcal/mol, bigger than those of alcohols. It could probably be related to duplication of O-...Na^+ intermolecular interactions between H_3PO_4 and NADPH.

Also, in the case of absorption of AsH_3 species by NADPH, the energy difference is -53.03 kcal/mol (about -30 kcal/mol bigger than alcohols), which makes this process very favorable given thermodynamics (compared to the alcohols and H_3PO_4). It indicates that AsH_3 might form a powerful complex system with NADPH that turns off its cycle. Finally, in the case of free Fe(II) ion, this species could be absorbed by NADPH with an absorption energy of -161.59 kcal/mol (approximately -131 kcal/mol bigger than alcohols). On the one hand, such absorption energy might be favorable (thermodynamically) and could make this process nearly irreversible. On the other hand, the results of the geometrical studies show that during the absorption of Fe(II) ion, the phosphate bridge breaks, and NADPH splits into two separate parts. In this case, such significant energy release could be logical.

Table 2. The reactivity descriptors of NADPH molecule at B3LYP/6-311G(d, p) level of theory

Reactivity Descriptor	Reactivity Descriptor Energy (a.u.)	Reactivity Descriptor	Reactivity Descriptor Energy (a.u.)
Electron affinity (A)	0.06	Electronegativity (N)	0.15
Ionization potential (I)	0.19	Electrophilicity index (ω)	0.11
Global hardness (η)	0.06	HOMO energy	-0.18595
Softness (S)	7.74	LUMO energy	-0.05686

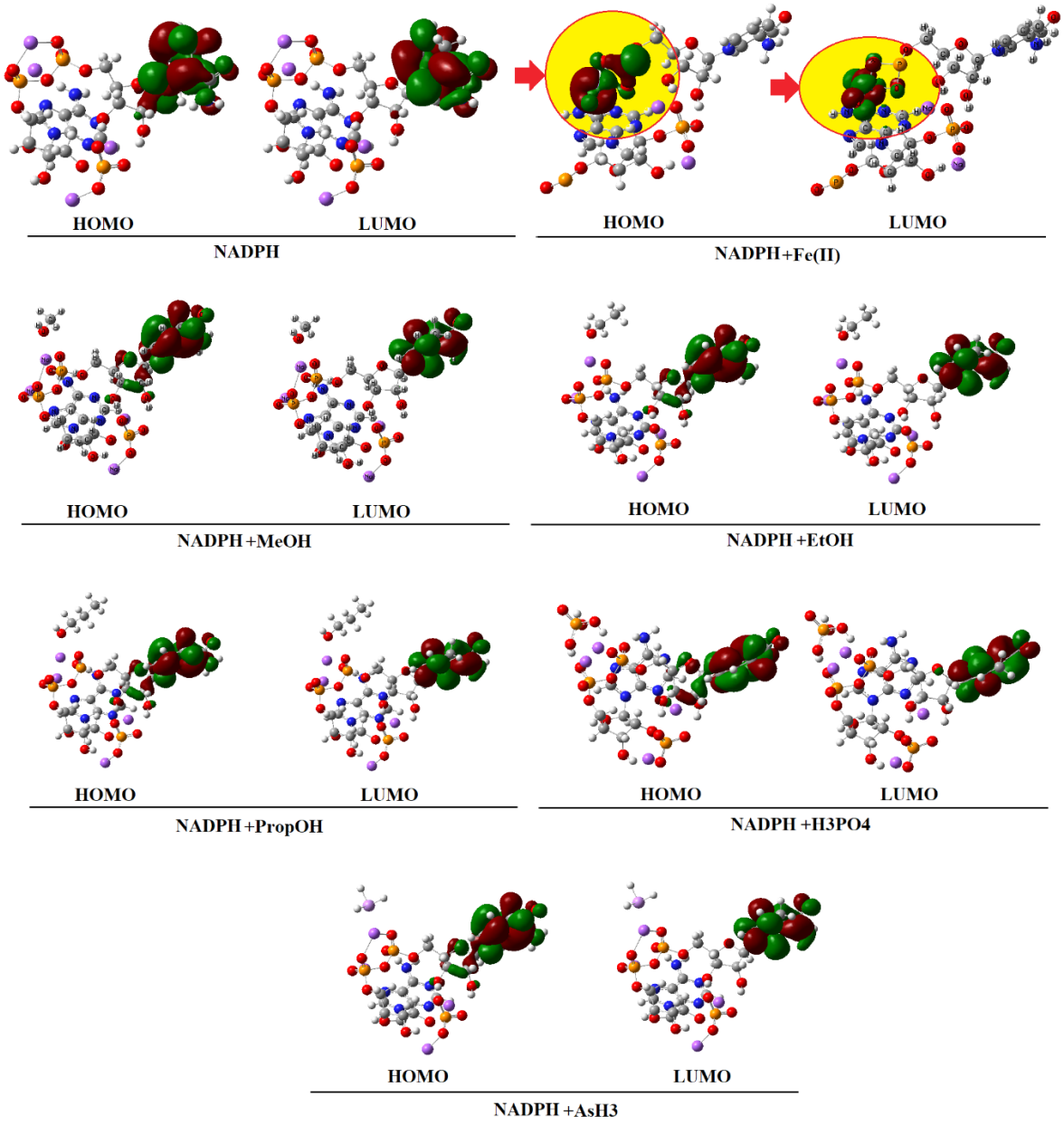

Figure 3. The fFMOs of the isolated NADPH and its complexes with the considered species

Besides the results mentioned above, it should be mentioned that the DFT approach is a trustable method to provide valuable insights into the substrate selectivity and chemical reactivity in terms of chemical concepts like the chemical potential (μ), softness(S), electronegativity (χ), electrophilicity index (ω), and chemical hardness (η). Moreover, using the Koopmans' theorem, ionization potential (I), electron affinity (A), hardness (η), electronegativity (χ), and softness (S), which are functions of the energy of HOMO and LUMO, some of the physiochemical properties of the molecules are predictable. The results in Table 2 show the reactivity parameters for the NADPH molecule. The results indicate that the HOMO–LUMO energy gap (E_g) is about -0.12909 a.u. which is relatively low. In detail, its low E_g results in low kinetic stability and, thus, high chemical reactivity.

NADPH's low ionization energy (I) (about 0.19 a.u.) shows that it is a highly reactive molecule. Moreover, the softness descriptor is applied to measure the chemi-

cal reactivity, which measures the capacity of an atom or a molecular fragment to gain electrons. The softness of NADPH (7.74 a.u.) reveals that it could be soft enough to give electron density to different types of atomic fragments (Table 2). Thus, it might be predicted that the softness of NADPH would be a parameter for increasing its reactivity for reducing chemical species. In addition, some of the recent reports confirm that decreasing the energy gaps could lead to easy transfers of electrons from HOMO to LUMO, which is very important for their molecular reactivity. Since the decrease in electronegativity index is related to an increase in inhibitive abilities [47], it has a higher inhibitory effect regarding its lower electronegativity. The smaller energy gap, lower electronegativity, and higher dipole moment, which might be required for the bioactivity effect of a molecule [47, 48], were observed in this case. In addition, previous reports have shown that electrophilicity (Table 2) is a suitable descriptor of biological activity [49, 50].

Given the frontier molecular orbitals (FMO) theory (Figure 3), it is observed that except for Fe(II) case, both the highest occupied molecular orbital (HOMO) and the lowest unoccupied molecular orbital (LUMO) of the systems are localized on the nicotinamide part of NADHP. However, in the Fe(II)-NADPH system, both HOMO and LUMO are localized on the phosphate bridge. It shows that significant changes occur in this system during the absorption of Fe(II) by NADPH. The electron exchange site is transferred from the nicotinamide part to the phosphate bridge. This issue would be another proof of destruction or at least considerable changes in the structure of NADPH after interaction with free Fe(II) compared to the other considered species.

Conclusion

In conclusion, the results of the PES studies indicate that adsorption of methanol, ethanol, normal propanol, and H_3PO_4 by NADPH release -23.19, -23.03, -23.30, and -35.04 kcal/mol energy, respectively, while, adsorption of arsine by this natural electron generator releases a -53.03 kcal/mol energy. Also, the free Fe(II) ion could interact with NADPH with an absorption energy of -161.59 kcal/mol (about -131 kcal/mol bigger than alcohols). Such absorption energy would be thermodynamically favorable enough to make this process approximately irreversible. Moreover, the results of the geometrical investigations indicate that during the absorption of free Fe(II) ions, the phosphate bridge of NADPH splits this molecule into two separate fragments. The free Fe(II) ion could destroy the NADPH molecule.

Finally, the results of the FMO calculations show that during the absorption of free Fe(II) ion by NADPH, both HOMO and LUMO are replaced from the nicotinamide part to the phosphate bridge (unlike most of the other cases containing alcohols and phosphoric acid). It could be considered another proof of significant changes in NADPH structure after its interaction with free Fe(II). Thus, free Fe(II) ions could turn off the NADPH natural electron generator and destroy its structure.

Ethical Considerations

Compliance with ethical guidelines

There were no ethical considerations to be considered in this research.

Funding

This research was taken from the PhD dissertation of Seyyed Amir Siadati, approved by Department of Medicinal Chemistry, School of Pharmacy, Mazandaran University of Medical Sciences, that was funded by the Mazandaran University of Medical Sciences Research Council (Grant No.: 18619).

Authors contribution's

All authors equally contribute to preparing all parts of the research.

Conflict of interest

The authors declared no conflict of interest.

Acknowledgements

The authors are grateful to Rezvan Yazdian Robati for her support.

References

[1] Kuchcinski G, Patin L, Lopes R, Leroy M, Delbeuck X, Rollin-Sillaire A, et al. Quantitative susceptibility mapping demonstrates different patterns of iron overload in subtypes of early-onset Alzheimer's Alzheimer's disease." Eur Radiol. 2023; 33(1):184-95. [DOI:10.1007/s00330-022-09014-9] [PMID]

[2] Tam E, Sung HK, Lam NH, You S, Cho S, Ahmed SM, et al. Role of mitochondrial iron overload in mediating cell death in H9c2 Cells. Cells. 2022; 12(1):118. [DOI:10.3390/cells12010118] [PMID]

[3] Foley PB, Hare DJ, Double KL. A brief history of brain iron accumulation in Parkinson disease and related dis-

orders. J Neural Transm (Vienna). 2022; 129(5-6):505-20. [DOI:10.1007/s00702-022-02505-5] [PMID]

[4] Kazemi Shariat Panahi H, Dehhaghi M, Heng B, Lane DJR, Bush AI, Guillemin GJ, et al. "Neuropathological mechanisms of β-N-Methylamino-L-Alanine (BMAA) with a focus on iron overload and ferroptosis." Neurotox Res. 2022; 40(2):614-35. [DOI:10.1007/s12640-021-00455-6] [PMID]

[5] Kolarova H, Tan J, Strom TM, Meitinger T, Wagner M, Klopstock T. Lifetime risk of autosomal recessive neurodegeneration with brain iron accumulation (NBIA) disorders calculated from genetic databases. EBioMedicine. 2022; 77:103869. [DOI:10.1016/j.ebiom.2022.103869] [PMID]

[6] Tavakoli S, Ebrahimzadeh MA, Sameni F, Biparva P, Mohammadi H, Ziar A, et al. "Excess iron ion reduction in a thalassemia model using silver nanoparticles modified by the tannin fraction of Myrtus communis extact." Nanomed Res J. 2020; 5(4):355-63. [DOI:10.22034/NMRJ.2020.04.007]

[7] Zhao Q, Ge Z, Fu S, Wan S, Shi J, Wu Y, et al. DNA methylation plays an important role in iron-overloaded Tibetans. Genes Genet Syst. 2022; 97(2):55-66. [DOI:10.1266/ggs.21-00006] [PMID]

[8] Kavitha B, Sravanthi M, Saritha Reddy P. Studies on DNA binding, cleavage, molecular docking, antimicrobial and anticancer activities of Cr (III), Fe (III), Co (II) and Cu (II) complexes of o-vanillin and fluorobenzamine Schiff base ligand. Appl Organomet Chem. 2022; 36(3):e6531. [DOI:10.1002/aoc.6531]

[9] Wang X, Li Y, Han L, Li J, Liu C, Sun C. Role of flavonoids in the treatment of iron overload. Front Cell Dev Biol. 2021; 9:685364. [DOI:10.3389/fcell.2021.685364] [PMID]

[10] Hashemi Z, Ebrahimzadeh MA, Biparva P, Mortazavi-Derazkola S, Goli HR, Sadeghian F, et al. "Biogenic silver and zero-valent iron nanoparticles by feijoa: biosynthesis, characterization, cytotoxic, antibacterial and antioxidant activities. Anticancer Agents Med Chem. 2020; 20(14):1673-87. [DOI:10.2174/1871520620666200619165910] [PMID]

[11] Bruzzese A, Martino EA, Mendicino F, Lucia E, Olivito V, Bova C, et al. "Iron chelation therapy." Eur J Haematol. 2023; 110(5):490-7. [DOI:10.1111/ejh.13935] [PMID]

[12] Hashemi Z, Ebrahimzadeh MA, Biparva P. Naked eye chemosensor and In vivo chelating activity of iron (III) by bromopyridine quinoxaline (BPQ). J Fluoresc. 2022; 32(5):1669-78. [DOI:10.1007/s10895-022-02893-7] [PMID]

[13] Eberle D, Ullmann P, Werck-Reichhart D, Petersen M. cDNA cloning and functional characterisation of CYP98A14 and NADPH: Cytochrome P450 reductase from Coleus blumei involved in rosmarinic acid biosynthesis. Plant Mol Biol. 2009; 69(3):239-53. [DOI:10.1007/s11103-008-9420-7] [PMID]

[14] Wang Y, Zhou S, Li R, Liu Q, Shao X, Zhu L, et al. Reassessing acetyl-CoA supply and NADPH availability for mevalonate biosynthesis from glycerol in Escherichia coli. Biotechnol Bioeng. 2022; 119(10):2868-77. [DOI:10.1002/bit.28167] [PMID]

[15] Escobar-Morreale HF. Iron metabolism and the polycystic ovary syndrome. Trends Endocrinol Metab. 2012; 23(10):509-15. [DOI:10.1016/j.tem.2012.04.003] [PMID]

[16] Kotla NK, Dutta P, Parimi S, Das NK. The role of ferritin in health and disease: Recent advances and understandings. Metabolites. 2022; 12(7):609. [DOI:10.3390/metabo12070609] [PMID]

[17] Mathew M, Sivaprakasam S, Phy JL, Bhutia YD, Ganapathy V. Polycystic ovary syndrome and iron overload: Biochemical link and underlying mechanisms with potential novel therapeutic avenues. Biosci Rep. 2023; 43(1):BSR20212234. [DOI:10.1042/BSR20212234] [PMID]

[18] Petrat F, Paluch S, Dogruöz E, Dörfler P, Kirsch M, Korth HG, et al. "Reduction of Fe (III) ions complexed to physiological ligands by lipoyl dehydrogenase and other flavoenzymes in vitro: implications for an enzymatic reduction of Fe (III) ions of the labile iron pool." J Biol Chem. 2003; 278(47):46403-13. [DOI:10.1074/jbc.M305291200] [PMID]

[19] Cher M, Davidson N. The kinetics of the oxygenation of ferrous iron in phosphoric acid solution. J Am Chem Soc. 1955; 77(3):793-8. [DOI:10.1021/ja01608a086]

[20] Reinke LA, Moore DR, Rau JM, McCay PB. Inorganic phosphate promotes redox cycling of iron in liver microsomes: Effects on free radical reactions. Arch Biochem Biophys. 1995; 316(2):758-64. [PMID]

[21] Funkhouser EA, Ackermann R. Nitrate reductase from Chlorella vulgaris. Reaction with manganese (III) pyrophosphate and with ferric o-phenanthroline. Eur J Biochem. 1976; 66(2):225-8. [DOI:10.1111/j.1432-1033.1976.tb10511.x] [PMID]

[22] Minotti G, Ikeda-Saito M. Bovine heart microsomes contain an Mr = 66,000 non-heme iron protein which stimulates NADPH oxidation. J Biol Chem. 1991; 266(30):20011-7. [DOI:10.1016/S0021-9258(18)54885-7] [PMID]

[23] Minotti G, Ikeda-Saito M. Fe(II) oxidation and Fe(III) incorporation by the M(r) 66,000 microsomal iron protein that stimulates NADPH oxidation. J Biol Chem. 1992; 267(11):7611-4. [DOI:10.1016/S0021-9258(18)42559-8] [PMID]

[24] Sijmons PC, van den Briel W, Bienfait HF. "Cytosolic NADPH is the electron donor for extracellular Fe reduction in iron-deficient bean roots." Plant Physiol. 1984; 75(1):219-21. [DOI:10.1104/pp.75.1.219] [PMID]

[25] Ahmed A, Domingo, L. R. Structure, reactivity, nonlinear optical properties and vibrational study of 5-thioxo-1, 4-thiazaolidin-3-one and 5-thioxo-1, 4, 2-thiazasilolidin-3-one (silicon vs. carbon). A DFT Study. Silicon. 2019; 11(4):2135-47. [Link]

[26] Kącka-Zych A, Jasiński R. Unexpected molecular mechanism of trimethylsilyl bromide elimination from 2-(trimethylsilyloxy)-3-bromo-3-methyl-isoxazolidines. Theor Chem Acc. 2019; 138:81. [Link]

[27] Rad AS, Ayub, K. Ni adsorption on Al12P12 nanocage: A DFT study. J Alloys Compd. 2016; 678:317-24. [DOI:10.1016/j.jallcom.2016.03.175]

[28] Vessally E, Siadati SA, Hosseinian A, Edjlali L. Selective sensing of ozone and the chemically active gaseous species of the troposphere by using the C20 fullerene and graphene segment. Talanta. 2017; 162:505-10. [DOI:10.1016/j.talanta.2016.10.010] [PMID]

[29] Domingo LR, Ríos-Gutiérrez M, Pérez P. A molecular electron density theory study of the participation of tetrazines in aza-Diels-Alder reactions. RSC Adv. 2020; 10(26):15394-405. [DOI:10.1039/D0RA01548B] [PMID]

[30] Siadati SA. Effect of steric congestion on the stepwise character and synchronicity of a 1, 3-dipolar reaction of a nitrile ylide and an olefin. J Chem Res. 2015; 39(11):640-4. [DOI:10.3184/174751915X14448371200600]

[31] Bondarchuk SV. Impact sensitivity of aryl diazonium chlorides: Limitations of molecular and solid-state approach. J Mol Graph Model. 2019; 89:114-121. [DOI:10.1016/j.jmgm.2019.03.008] [PMID]

[32] Siadati A. A theoretical study on the possibility of functionalization of C20 fullerene via its Diels-Alder reaction with 1, 3-butadiene. Lett Org Chem. 2016; 13(1):2-6. [Link]

[33] Shiri P, Amani AM, Mayer-Gall T. A recent overview on the synthesis of 1, 4, 5-trisubstituted 1, 2, 3-triazoles. Beilstein J Org Chem. 2021; 17:1600-28. [DOI:10.3762/bjoc.17.114] [PMID]

[34] Siadati SA. A Theoretical study on stepwise- and concertedness of the mechanism of 1,3-dipolar cycloaddition reaction between tetra amino ethylene and trifluoro methyl Azide. Comb Chem High Throughput Screen. 2016; 19(2):170-5. [DOI:10.2174/1386207319666151216145408] [PMID]

[35] Bekhradnia AR, Arshadi S, Siadati SA. 1, 3-Dipolar cycloaddition between substituted phenyl azide and 2, 3-dihydrofuran. Chemical Papers. 2014; 68:283-90. [Link]

[36] Kącka-Zych, A, Jasiński, R. Understanding the molecular mechanism of the stereoselective conversion of N-trialkylsilyloxy nitronates into bicyclic isoxazoline derivatives. New J Chem. 2021; 45(21):9491-500. [DOI:10.1039/D1NJ01198G]

[37] Siadati SA, Alinezhad, M. A theoretical study on the functionalisation process of C18NB fullerene through its open [5, 5] cycloaddition with 4-pyridine nitrile oxide Prog React Kinet Mech. 2015; 40(2):169-76. [DOI:10.3184/146867815X14262612008408]

[38] Kącka-Zych A, Jasiński R. A DFT study on the molecular mechanism of the conjugated nitroalkenes polymerization process initiated by selected unsaturated nucleophiles. Theor Chem Acc. 2020; 139(7):119. [Link]

[39] Siadati SA, Davoudi S, Soheilizad M, Firoozpour L, Payab M, Bagherpour S, et al. The synthesis and the mechanism of a five-membered ring formation between an isothiocyanate and an amide leading to the yield of Enzalutamide anticancer API; A joint experimental and theoretical study J Mol Struct. 2023; 1280:135057. [DOI:10.1016/j.molstruc.2023.135057]

[40] Mlostoń G, Kula K, Jasiński R. A DFT study on the molecular mechanism of additions of electrophilic and nucleophilic carbenes to non-enolizable cycloaliphatic thioketones. Molecules. 2021; 26(18):5562. [DOI:10.3390/molecules26185562] [PMID]

[41] Cao X, Wu L, Zhang J, Dolg M. Density functional studies of coenzyme NADPH and its oxidized form NADP+ : Structures, UV-Vis spectra, and the oxidation mechanism of NADPH. J Comput Chem. 2020; 41(4):305-16. [DOI:10.1002/jcc.26103] [PMID]

[42] Singh P, Chaubey S, Singh C, Singh S, Yadav RK, Singh AP, et al. "Polystyrene-based eosin-Y as a photocatalyst for solar light-mediated NADH/NADPH regeneration and organic transformations." React Chem Eng. 2023; 8(5):1072-82. [DOI:10.1039/D2RE00203E]

[43] Keshavarz F. Molecular level insights into the direct health impacts of some organic aerosol components. New J Chem. 2021; 45(15):6709-23. [DOI:10.1039/D1NJ00231G]

[44] Wu X, Zhang Z, Soleymanabadi H. Substituent effect on the cell voltage of nanographene based Li-ion batteries: A DFT study. Solid State Commun. 2020; 306:113770. [DOI:10.1016/j.ssc.2019.113770]

[45] Becke AD. Density-functional exchange-energy approximation with correct asymptotic behavior. Phys Rev A Gen Phys. 1988; 38(6):3098-100. [PMID]

[46] Lee C, Yang W, Parr RG. Development of the Colle-Salvetti correlation-energy formula into a functional of the electron density. Phys Rev B Condens Matter. 1988; 37(2):785-9. [DOI:10.1103/PhysRevB.37.785] [PMID]

[47] Delchev VB, Nenkova MV. Theoretical modeling of the ground state intramolecular proton transfer in cytosine: DFT level study. Acta Chim. Slov. 2008; 55(1).132-7. [Link]

[48] Babu S, Nagarajan SK, Sathish S, Negi VS, Sohn H, Madhavan T. Identification of potent and selective JAK1 lead compounds through ligand-based drug design approaches. Front Pharmacol. 2022; 13:837369. [PMID]

[49] Parthasarathi R, Subramanian V, Roy DR, Chattaraj PK. Electrophilicity index as a possible descriptor of biological activity. Bioorg Med Chem. 2004; 12(21):5533-43. [PMID]

[50] Mohammadi M, Siadati SA, Ahmadi S, Habibzadeh S, Poor Heravi MR, Hossaini Z, Vessally E. Carbon fixation of CO2 via cyclic reactions with borane in gaseous atmosphere leading to formic acid (and metaboric acid); A potential energy surface (PES) study. Front Chem. 2022; 10:1003086. [DOI:10.3389/fchem.2022.1003086] [PMID]